DISCUSSIONS

CASE WESTERN RESERVE UNIVERSITY UNDERGRADUATE RESEARCH JOURNAL

HEARING LOSS PHENOMENON

in Usher Syndrome 1: Protein Profiling of the Cochlea, Using Proteomic Methodologies

Rebecca Levinson

CELL CYCLE EFFECTS

of Simultaneous Treatment with U0126 MEK Inhibitor and Nocodazole

Natalie Pyatka

BREATH PLAY:

Sexual and Autoerotic Asphyxiation

Liz Oakley

VOLUME 6, ISSUE 1

FALL 2009

CASE WESTERN RESERVE UNIVERSITY EST. 1826

DISCUSSIONS

CASE WESTERN RESERVE UNIVERSITY UNDERGRADUATE RESEARCH JOURNAL

TABLE OF CONTENTS

2009-2010 Editorial Board

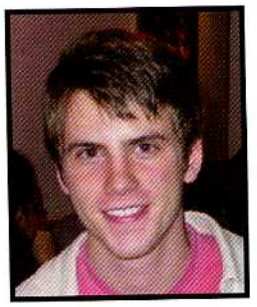

SEAN YELDELL
Editor-in-Chief

PYONE THI
Managing Editor

HIMANSHU SHARMA
Business Manager

TOM TEE
Web Design

EMILY MOORE
Advertising Co-Chair

BHARATHI MUTHUSAMY
Advertising Co-Chair

REVIEWERS

Laura Bryant
Megan Carl
Angela Carlson
Leah Dodson
Steve Ehret
G. Connor Evans
Kim Girosky
Brian Hysell
Natalie Pyatka
Michelle Williams

ADVISOR
Sheila Pedigo, Ph.D.

WEB ADVISOR
Bethany Pope

COPY EDITORS
Leah Dodson
Kim Girosky
Pyone Thi

COVER ILLUSTRATION
Sean Yeldell

Letter from the Editors

Dear Reader,

Welcome to a new issue of *Discussions*!

Over the past few years we have been gradually increasing the quality of the journal -- in 2007 we introduced a higher quality binding, in 2008 we moved to a full color interior, and with this issue we are enhancing the journal with a more durable and professional 70# paper.

Additionally, our Web Design Officer, Tom Tee, has revamped our website and relocated us to discussions.case.edu. Expect to see that up and running at the time that this journal is released, and send your feedback to discussions@case.edu.

Liz Oakley's *Breath Play: Sexual and Autoerotic Asphyxiation* is the second piece of research published from a student outside of the CWRU undergraduate community in the history of *Discussions*. The journal remains run by CWRU students, printed and distributed in the CWRU area, and composed primarily by research of CWRU students. However, if you have any friends or colleges at other schools who are not fortunate enough to have the opportunity to publish in an undergraduate journal of their own, encourage them to submit their research here.

We are grateful for the continued assistance of Dr. Sheila Pedigo and Bethany Pope in the SOURCE office, as well as the continued support of Media Board. We encourage you to follow the links at the back of this issue to visit their web pages and learn more about both organizations.

The deadline for the next spring's issue will be a few short weeks into the beginning of the semester, so start compiling your articles for submission now!

We hope you enjoy the range of articles presented here, and we hope to see this journal continue to ignite scholarly discussion across the campus.

Sincerely,
Sean Yeldell and Pyone Thi
Editor-In-Chief and Managing Editor

Hearing Loss Phenomenon in Usher Syndome 1: Protein Profiing of the Cochlea, Using Proteomic Methodologies

-Rebecca Levinson-

Rebecca Levinson is a fourth year student studying biology and philosophy at CWRU. Outside of the classroom she is active in the University Program Board, and the National Residence Hall Honorary. After the conclusion of her undergraduate experience she plans to go to graduate school.

~Acknowledgements~

I would like to thank Mark Chance and Giridharan Golkurangan for helping me design and execute this project. Thank you to Jennifer Burgoyne, Katy Lundberg, Chao Yuan, Danielle Schlatzer, and Elizabeth Yohannes for aiding me with sample preparation and answering all my questions, and Gaurav Rana for helping me with bioinformatics. Thanks to Kumar Alagramam for providing me with mouse cochlea. I would also like to thank my advisor Robin Snyder for encouraging me during the completion of this project. I would like to thank Joan Schenkel and Shannon Swiatkowski for finding me funding. Finally, I would like to thank the National Institutes of Health for partial funding for this work.

ABSTRACT

Hearing loss usually results from the abnormal development of, or injury to, the "hair cells" in the cochlea (inner ear). Usher syndrome, a type of deafness, is characterized by the degeneration of hair cells due to genes involved in HH1 (Geller et al, 2009). Mouse mutants that simulate Usher syndrome have served as an excellent model to understand the basis for HHI. Prior work has identified networks of proteins in the cochlea, specifically those associated with cellular degeneration as factors that contribute to Usher syndrome (Chance et al). Protein profiling, using gel-based approaches like 2D differential expression analysis (2D DIGE), has shed light on the possible roles of different proteins including cochlin (Chance et al). That data has suggested that Cochlin and its isoforms are very much involved in the mechanism of hearing loss (Chance et al). A "shotgun" approach of cleaving proteins into peptides prior to their analysis with liquid chromatography-mass spectrometry (LC-MS) technology is a more sensitive alternate approach. The goal is to (a) profile the Cochlear proteome (protein compendium) using proteomic methodologies such that we can decipher the role of cochlin and its related proteins and (b) isolate and characterize Cochlin precursor proteins such that more can be determined about its role in hearing loss.

INTRODUCTION

Usher syndrome is a degenerative disease that causes ear and eye problems in humans (NIDCD, 2008). There are several types of usher syndrome, USH1F, being the most common. Usher syndrome is responsible for about 3-6% of the cases of deafness in the United States (NIDCD, 2008). The most common eye degeneration from Usher syndrome is retinitis pigmentosa, or tunnel vision (HHIRR, 2009). Almost 4 out of every 100,000 babies are born with Usher syndrome (NIDCD, 2008). Babies with Usher syndrome are either born deaf or will become deaf in the first year of their life (Genetics Home Reference, 2009). Difficulty walking and sitting up often accompanies Usher syndrome, as balance is controlled by the inner ear.

There is significant research trying to identify the gene defects associated with Usher syndrome (Genetics Home Reference, 2009). Recently, it was determined that a mutation of the PCDH15 gene which codes for the protocadherin15 protein is important in Usher syndrome (Ahmed et al, 2008 and NCBI, 2009).

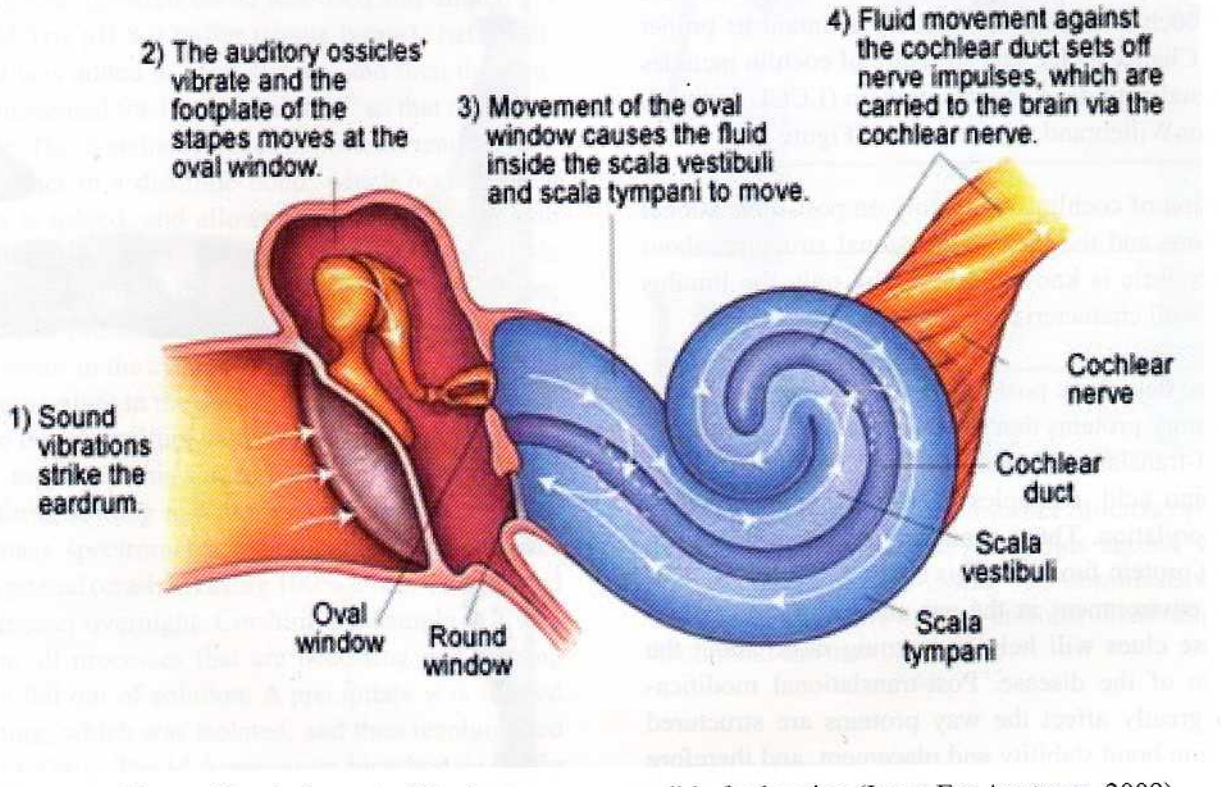

Figure 1: The cochlea is the part of the inner ear responsible for hearing (Inner Ear Anatomy, 2009).

The inner ear cochlea is made up of several types of cells, including hair cells, which play an important role in hearing. If these hair cells are damaged, it will affect the ability to hear. During the progression of Usher syndrome, the hair cells and other cochlear cells gradually begin to self-destruct by an unknown mechanism. Eventually a hole is left in the cochlea (Figure2).

The identification of this phenomenon prompted our approach, as the gene mutations have identifiable consequences in a specific tissue. A proteomic study on the tissue affected by the mutation would allow us to see the changes in the amount of various proteins in the cell during the progression of the disease, which can connect the histology with a specific molecular pathology (Chance et al). Proteomics is the study of the structure, abundance, interaction, and function of all proteins in a sample. The proteome is the collection of all proteins present in a tissue or organ and can change due to environmental conditions or health status. For example, the proteome of one mouse may dramatically change in a healthy mouse compared to one with a specific disease. There is only one genome for the cell, but the proteome can vary depending on age or environmental factors. We have chosen to profile the proteome because it will permit us to analyze many of the proteins in the inner ear including cochlin, one of the major auditory proteins. Profiling the proteome means creating a detailed list of which proteins are the most common in the cochlea, and which genes and processes these proteins are associated with. We also used a comparative method in our profiling, in which we looked at the difference in the proteomes between normal mice and those having Usher syndrome due to a mutation in PCDH15. This provides us with information about the specific proteins that are associated with deafness.

We discovered a large number of proteins that were present in the cochlea. After obtaining a general idea of the protein environment of the cochlea we chose to focus our attention on cochlin. Cochlin is hypothesized to be extremely important in the structure of the inner ear (Chance et al). It is a structural protein secreted into the intercellular matrix and is theorized to bind collagen and other structural proteins to provide a specific molecular archi-

tectural structure for the ear (Nagy et al. 2008). Cochlin is found in multiple isoforms, which theoretically affect the ability of cochlin to help the cochlea maintain its proper structure (Chance et al). The structure of cochlin includes a short signal peptide, a limulus domain (LCCL domain), and two vonWillebrand type A factors (Figure 3).

Our attention of cochlin was mainly on post-translational modifications and the three dimensional structure, about which very little is known. In cochlin, only the limulus domain is well characterized.

We can also determine post-translational modifications of major auditory proteins that are in one sample and not the other. Post-translational modifications are small changes to the amino acid, examples of which are methylation or phosphorylation. These changes are known to lead to changes in protein function. This could help give us clues about the environment in the ear under different conditions. These clues will help in learning more about the progression of the disease. Post-translational modifications can greatly affect the way proteins are structured by disrupting bond stability and placement, and therefore how they function.

MATERIALS AND METHODS

An Ames Waltzer (av) mouse was used as a model for Ushers syndrome. The av mouse has an induced mutation in the protocadherin15 gene, which causes deafness, making it a suitable model for human deafness. The cochleas were excised from the ears of a mouse with the induced mutation, and from a mouse without the mutation both at the age of 30 days. The cochlear tissue was stored in 300μL of 25mM Tris pH 8.8 buffer to allow for a minimal amount of protein degradation during storage and was then homogenized.

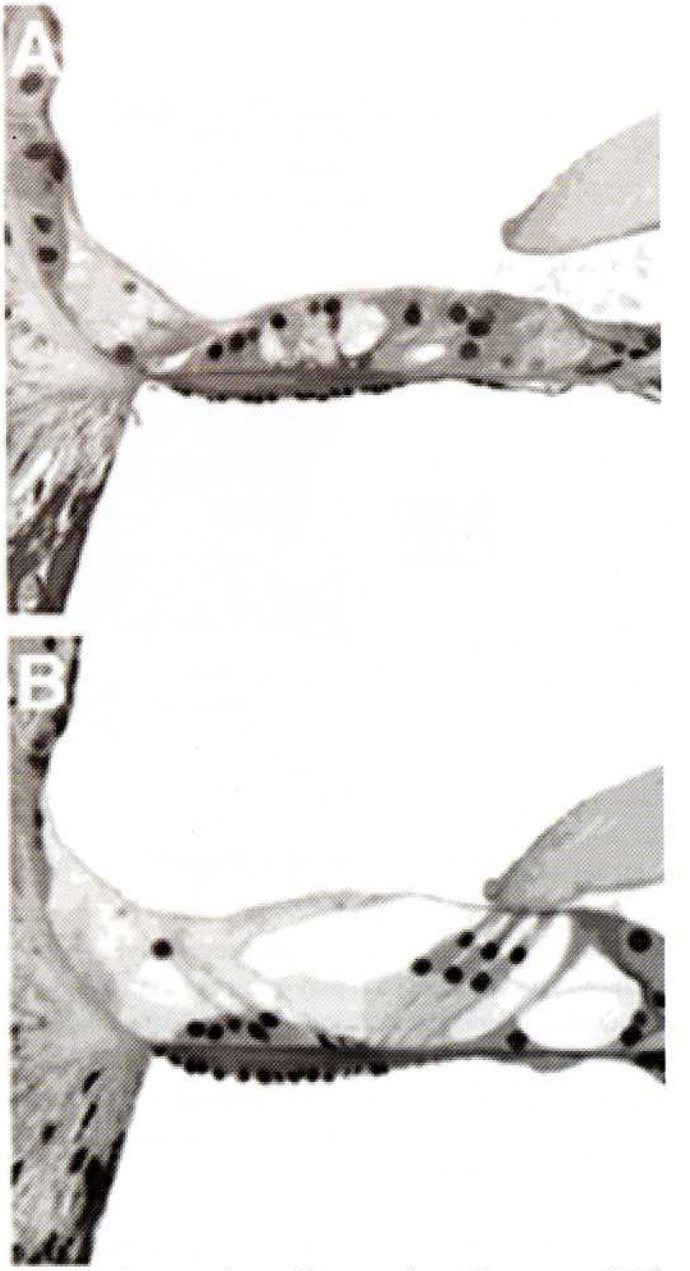

Figure 2: A comparison of organ of corti in a normal (A) and av (B) mouse (Chance et al).

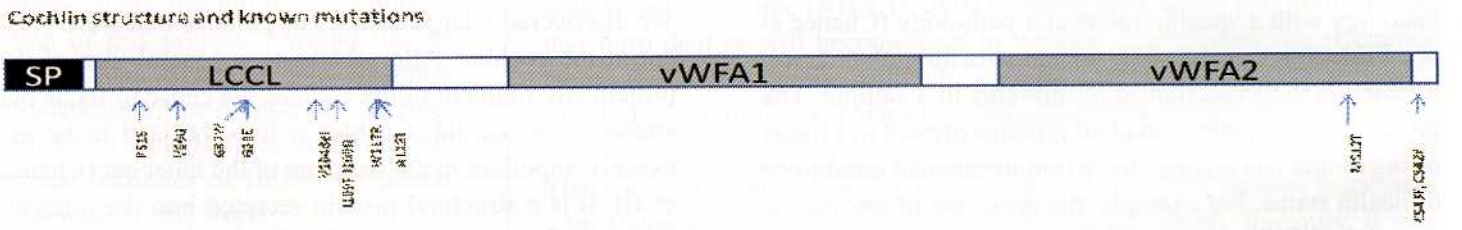

Figure 3: The structure of cochlin with the known human mutations in the amino acid sequence (Robertson et al., 2008).

For the first approach, known as "shotgun" proteomics, 35µL of the homogenized tissue was used and diluted 1:1 with 25mM Tris pH 8.0 buffer (tissue lysate). 1µL of dithiothreitol was added to each sample, and then the samples were incubated for 10 minutes at 56° so that reduction could occur. The cysteine residues in proteins tend to bond with each other in a disulfide bond, which occurs when the protein is folded, and allows the protein to maintain its tertiary conformation. Reduction breaks the disulfide bonds, helping to unfold the protein. After the incubation, 8µL of 550µM Iodoacetamide was used for alkylation of the sulfur atoms in the cysteine residues before incubating at room temperature in the dark for 45 minutes. Alkylation makes it so that the sulfurs on the cysteine residues cannot bind back together. This forces the protein to stay in an unfolded form, leading to a more complete digestion and stronger mass spectrometry identification. The samples were precipitated (crashed) using 100% ethanol and stored in a -20° freezer overnight. Crashing the sample is a way of stopping all processes that are occurring and making the protein fall out of solution. A precipitate was formed after crashing, which was isolated, and then resolubilized in 100µL of 8M in 25mM Ammonium bicarbonate buffer pH 8.0. The reduction and alkylation were repeated before digesting the sample using a tryptic digest. A tryptic digest enzymatically cleaves protein using the enzyme trypsin. Trypsin cuts the peptide bond at the C-terminal end of each lysine and argenine, unless followed by a proline. We took the product of our digest, and performed a clean up using a C-18 chromatography column to remove any salts present that would affect the charges of the peptide. We then added .01% formic acid, and transferred to HPLC vials for nano LC-MS/MS.

In a second approach, we loaded a 4-20% gradient SDS-Page gel with 15µL of each sample cell protein extract. This gel separates the proteins by molecular weight, allowing the smallest proteins to travel the farthest through the gel, while the largest proteins travel the least distance. The SDS detergent binds the proteins and makes them negatively charged. A current is run through the gel to help the fragments move and settle throughout the gel. This gel ran at 120V and was then stained using coomasie blue dye, which helps visualize the proteins. The gel was destained and cut into bands. Each of these bands was digested separately using a tryptic digest. This gave us

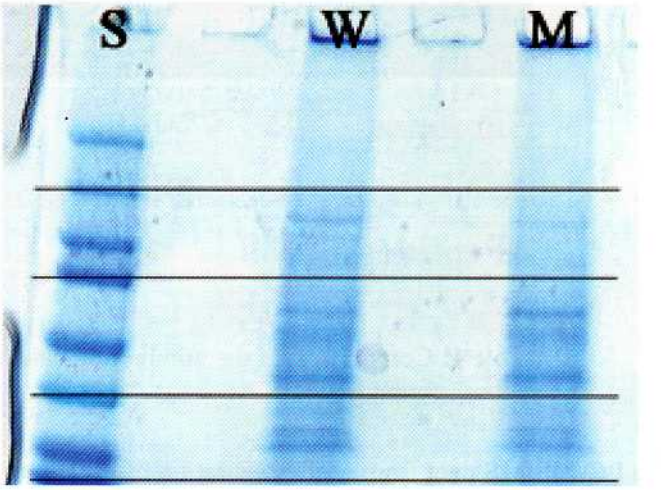

Figure 4: Light and fluorescence microscopy of electrospun poly(caprolactone) scaffolds seeded with green fluorescent protein expressing 3T3 fibroblasts via electrostatic spraying, showing the uniform distribution of cells throughout the matrix.

5 bands per sample (Figure 4). The five bands had molecular weights of 5-20kDa, 21-37kDa, 38-75kDa, 76-150kDa, 151-250kDa from the bottom of the gel to the top. Each of these digested bands had formic acid added, and was run though liquid chromatography tandem mass spectrometry (LC-MS/MS) and peptide separation.

Nano-LC-MS/MS is a set of instruments that allow a sample to be analyzed using a combination of liquid chromatography and mass spectrometry at a high resolution. When a sample is injected into the LC-MS/MS, it is pushed into a chromatography column where the peptides bind. Then a series of liquids are run through the column starting with inorganic and increasing in organic concentration. The peptides are released from the column based on their charge and chemical properties and leave the column entering the ionization chamber of the MS. A chromatograph is generated showing the intensity of a molecule versus the mass per charge (m/z) ratio of that molecule. The molecules are collided with gas molecules to break the peptide bonds. The change in the mass per charge ratio as peptides are removed gives a probable sequence. An MS2 is generated detailing the breakdown of the peptide.

	Wildtype Only	Mutant Only	Both	Total
Proteins	45	7	286	331
Peptides	789	232	867	1888

Table 1: Comparison of the number of proteins and peptides found in only one of the samples as well as those found in both.

The LC-MS/MS data from each preparation of each sample was run through a series of computer programs to identify the proteins present. The computer programs used were Mascot Daemon, Scaffold, and Babelomics. Mascot Daemon used the files generated from the mass spectrometry to generate a redundant list of proteins present in the sample. To avoid redundancies and increase statistical reliability, we analyzed the same files in Scaffold. Scaffold produced a list of protein IDs that identify which gene a protein comes from. These IDs can be put into Babelomics, a program that identifies the genes involved in specific pathways and creates maps indicating important types of processes.

To identify post-translational modifications, data from mouse deafness studies that had been prepared in a 2D DIGE method was used. 2D DIGE is a gel procedure, in which the protein fragments are separated by isoelectric point and then by mass (Chance, 2008). This was done because 2D DIGE allows certain modifications, such as phosphorylations to be seen more clearly. Bioinformatic analysis allowed the identification of modifications on specific amino acid residues. The chromatographs and MS/MS spectra associated with each of these modifications were analyzed, eliminating the spectra that did not indicate a real modification.

RESULTS

The protein we saw in the greatest quantity in both the diseased and control mouse in both of the preparations was cochlin. There were a total of 331 proteins in the control sample and a total of 293 proteins in the diseased sample (Table 1).

We found 45 proteins and 789 peptides in the wildtype samples only. There were 7 proteins and 232 peptides that appeared only in the mutant sample. 286 proteins and 867 peptides appeared in both samples. We found several post-translational modifications on cochlin. Those that appear to be the most important are the 362 Lysine, which we found can be modified by an acetylation or a methylation, the phosphorylation on the 126 threonine, and the methylation on the 545 argenine.

In the control sample, growth and cell maintenance protein groups were important, as determined by bioinformatic analysis, and the proteins necessary appeared in greater concentration. The bioinformatic analysis was done by David, a program that generated the gene ontology (GO) groups that each protein fits into, and identifies the most probable group given the processes occuring in the cell. When the data was analyzed, we generated a diagram of the biological processes found in each of the samples.

The wildtype sample had biosynthetic and cellular metabolic pathways that were not found in the mutant. The number of protein partners participating in the process may account for some of the discrepancy between mutant and wildtype protein identifications. The mutant had cellular developmental, nitrogen compound metabolic, maturation, and death processes not seen in the wildtype. In particular, the diseased sample, the cell death pathway had a much greater prevalence.

Cochlin was represented by 1.15% of all spectra in the control and 1.6% of spectra in the mutant. It was the protein in greatest abundance in each sample. We also found the coverage of the cochlin sequence by each of the samples (Figure 6). Coverage is the amount of the amino acid sequence of the protein that we could identify.

The coverage of cochlin was 78%, but there was difficulty in finding the N-terminus of the protein. In analyzing the MS/MS spectra we found several modifications on cochlin. We annotated the original spectra in each case (Figure 7), as well as using Mascot Daemon to add significance to our results.

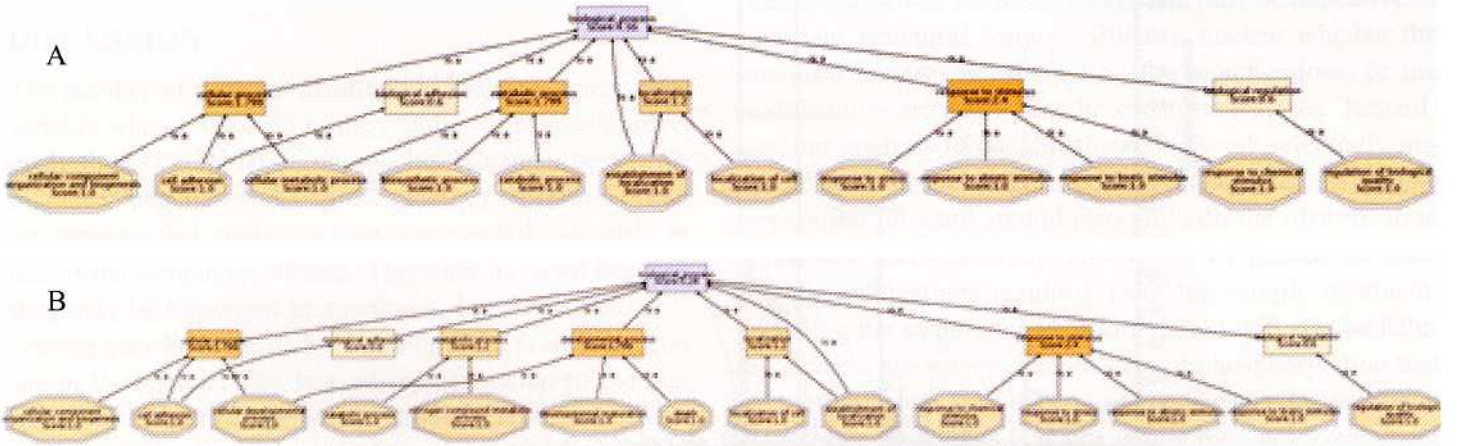

Figure 5: The biological processes represented by the proteins found in the cochlea of the wildtype mouse (A) and the processes represented by the mutant mouse (B).

Gene Symbol= Coch Cochlin

Control 434/552 amino acids (78.6% coverage)

Diseased 436/552 amino acids (78.9% coverage)

MPSSRIPALC LGAWLLLLLL PRFARAEGAV PIPVTCFTRG LDIRKEKADV
LCPGGCSLEE FSVFGNIVYA SVSSICGAAV HRGVIGTSGG PVRVYSLPGR
ENYSSVDANG IQSQMLSRWS ASFAVTKGKS STQEATGRAV STAHPPSGKR
LKKTPEKKTG MKDCKADIAF LIDGSFNIGQ RRFNLQKNFV GKVALMLGIG
TEGPHVGLVQ ASEHPKIEFY LKNFTSAKDV LFAIKEVGFR GGNSNTGKAL
KHTAQKFFTA DTGVRKGIPK VVVVFIDGWP SDDIEEAGIV AREFGVNVFI
VSVAKPIPEE LGMVQDVAFM DKAVCRNNGF FSYHMPNWFG TTKYVKPLVQ
KLCTHEQMMC SKTCYNSVMI AFLIDGSSSV GDSNFRLMLE FVSNIAKTFE
ISDIGAKIAA VQFTYDQRTE FSFTDYNTKE NVLAVLANIR YMSGGTATGD
ALAFTVRNVF GPIRDSPNKN FLVIVTDGQS YDDVRGPAAA AHDAGITIFS
VGVAWAPLDD LRDMASKPKE SHAFFTREFT GLEPIVSDVI RGICRDFLES
QQ

Green= Control & Diseased
Yellow= Control Only
Red= Diseased Only

Figure 6: Coverage of the cochlin sequence by sample.found in both.

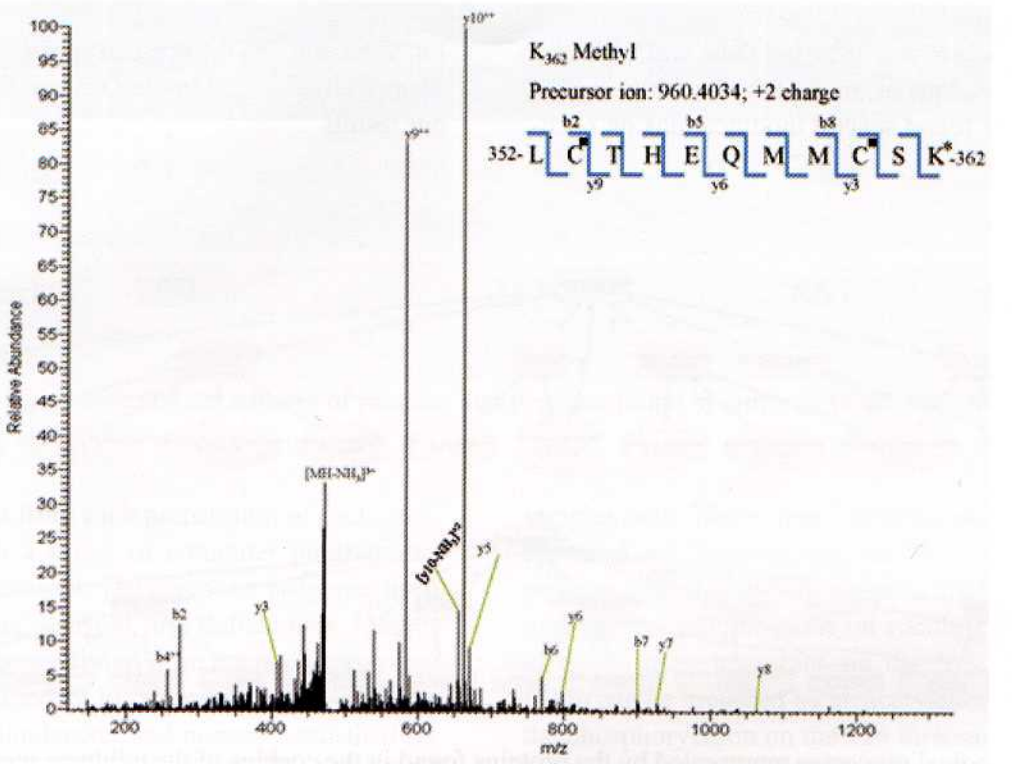

Figure 7: Sample MS2 spectra with notations to our results.

Peptide	Residue	Sequence	Approach
352-362	362	LCTHEQMMCSK*362	Gel Fractionation (Control)
182-192	182, 187, 192	R*182FNLQK■187NFVGK▲192	Gel Fractionation (Control)
158-181	159, 162, 175, 181	KT●159GNK▲162DCKADIAFLIDGS●175FNIGQR▲181	Shotgun (Control)
154-162	154, 162	T●154PEKKTGNK▲162	Shotgun (Control)
153-158	153, 157, 158	K■153TPEK■157K▲158	Gel Fractionation (Mutant)
352-362	362	LCTHEQMMCSK*362	Gel Fractionation (Mutant)
158-165	162	KTGNK*162DCK	Gel Fractionation (Mutant)
241-248	248	GGNSNTGK*248	Shotgun (Mutant)
542-552	545	GICR*545DFLESQQ	Gel Fractionation (Mutant)
154-162	154, 162	T●154PEKKTGNK▲162	Shotgun (Mutant)
154-165	158	TPEKK■158TGNKDCK	DIGE
119-129	126	WSASFAVT●126KGK	DIGE
352-362	362	LCTHEQMMCSK■	DIGE
■=Acetyl	▲=Dimethyl	*=Methyl	●=Phospho ♦=Trimethyl	

Table 2: Post-Translational modifications found on cochlin.

We attempted to correlate modifications to important structural features on the cochlin protein. This was done by looking at the structure of cochlin and the known mutation sites, and marking those that were within range to affect each other. We were left with three modifications that occurred near important structural sites of interest.

DISCUSSION

The number of proteins identified in the proteome is reasonable when compared to the number of proteins previously found by 2D DIGE approaches (Chance, 2008). We included "one hit wonder" proteins in our reporting. These are proteins that may have been represented only once in one of the sample repetitions. These are included because they may be important in a pathway, but the sample processing may have limited the amount of a protein we can see in the sample. The lack of representation of the one hit wonders may be due to our sample preparation affecting the protein and we would not want to discard important proteins or peptides due to flaws in our approach. This was also one of the reasons we used two complementary approaches. The shotgun digest and gel fractionation approaches treat the proteins in different ways. If one approach degrades a fragile protein, hopefully the other allows it to remain intact so it can be represented in the proteome. The proteins we expected to see most represented by both samples, cochlin, collagen, and various membrane proteins were highly represented. This is good because it tells us that our approach has not seriously destroyed the proteins. We cannot compare our results against previously published work, because the proteome of the cochlea has not yet been published. Following the completion of the wet lab work for this study, a new paper on how to reduce the remaining detergents in the sample, and therefore have a cleaner LC-MS/MS run, has been published (Wisniewski, 2009). Using this approach in the future and repeating the work done will add validity to our current results.

We looked at the sequence of cochlin after mapping it using Scaffold. This sequence was represented in the samples in a way that was consistent with what is known about cochlin. The N-terminus region was not represented in the mutant, which is consistent because cochlin has several different isoforms, mainly involving parts of the N-terminus being cleaved. In the normal mouse, a greater proportion of the N-terminus was represented, indicating that cochlin appears in normal mice in its more complete form. Neither of our preparations allowed us to see convincing coverage on the N-terminus that we hoped for, and this will hopefully also be increased by a new sample preparation protocol.

The modifications we found on cochlin may be indicative of important structural features. But it is unclear whether the structural features are disrupting the modifications, or the modifications are disrupting the structural features. Regardless, our analysis of cochlin showed several potentially important sites for the structure of the protein. The new sample preparation protocol should also aid with the identification of post-translational modifications as it will reduce the number of modifications resulting from the sample treatment. Enriching the sample for phosphorylation will also be helpful, as there are several known sites of phosphorylation that are thought to be important. A major obstacle to looking at post-translational modifications is that little is known about the importance of the methylation and acetylation modifications, which we found in several of our peptide chains.

A more in depth look at cochlin will help to reveal a lot, as it is so important in the ear, and is found in few other places in the body. Finding the binding partners of cochlin at different stages of degeneration will allow us to determine the environment in the cochlea at different times during the process. The binding partners will also be determined by the sequence of cochlin, and determining the cutting that leads to the sequences present during degeneration could be important in identifying factors in cochlear structural problems occurring during deafness. Using cochlin specific antibodies in an immune-precipitation approach will be a helpful next step, as it will allow us to affirm the cleavage points on the cochlin N-terminus.

The next steps in uncovering Usher syndrome are to do a micro-dissection and look at the protein changes in specific types of cells within the cochlea. Another logical step would be to look at the proteome of the eye during the course of degeneration. The similarities between the ear and the eye proteins will allow us to pinpoint what proteins are most significant in Usher syndrome 1 with a greater degree of confidence.

REFERENCES

Ahmed et al (2008). "Gene structure and mutant alleles of PCDH15: nonsyndromic deafness DFNB23 and type 1 Usher syndrome." *Hum Genet. 124*(3): 215-23.

Alagramam et al (2001). "Mutations in the novel protocadherin PCDH15 cause Usher syndrome type 1F". *Hum Mol Genet . 10,*(16):1709-1718

Alagramam et al. (2001) "The mouse Ames waltzer hearing-loss mutant is caused by mutation of Pcdh15, a novel protocadherin gene". *Nat Genet. 27*(1): 99-102.

Chance M, Chang J, et al. (Unpublished data) Case Western Reserve University, 10900 Euclid Ave, Cleveland, OH 44106, USA.

I. Nagy, M. Horváth, M. Trexler, G. Répássy, L. Patthy. (2004). "A novel COCH mutation, V104del, impairs folding of the LCCL domain of cochlin and causes progressive hearing loss". *J Med Genet. 41*(9): http://www.jmedgenet.com/cgi/content/full/41/1/e9.

I. Nagy, M. Trexler, L. Patthy. (2008). "The Second von Willebrand type A domain of cochlin has high affinity for type I, type II and type IV collagens". *FEBS Lett. 582*(29): 4003-4007.

Inner Ear Anatomy. Cochlin Fluids Laboratoy, Washington University. August 2009. http://oto2.wustl.edu/cochlea/intro1.htm

JR. Wisniewski, A Zougman, N. Nagaraj, M. Mann. (2008). "Universal Sample Preparation method for proteome analysis." *Nat Methods. 6*(5): 359-562.

N. Robertson et al. "A targeted Coch missense mutation: a knock-in mouse model for DFNA9 late onset hearing loss and vestibular dysfunction". Human Molecular Genetics. 17, 21. (2008): 3426-3434.

PCDH15 protocadherin 15 [Homo sapiens]. National Center for Biotechnology Information. February 2009. http://www.ncbi.nlm.nih.gov/sites/entrez?Db=gene&Cmd=retrieve&dopt=full_report&list_uids=65217&log$=genesensor4&logdbfrom=pubmed

SF. Geller et al. (2009). "CLRN1 is nonessential in the mouse retinal but is required for cochlear hair cell development". *PLoS Genet. 5*(8): Epub 2009 Aug 14.

Usher Syndrome & Retinitis Pigmentosa: Information & Referrals. 1999. Hereditary Hearing Impairment Resource Registry. June 2009. http://www.deafblind.com/nidcd.html.

Usher syndrome. (2009). Deafness Research Foundation. April 17, 2009. http://www.drf.org/hearingbalanceresearch.htm .

Usher syndrome. (2009). Genetics Home Reference. August 2009. http://ghr.nlm.nih.gov/condition=ushersyndrome.

Usher syndrome. (2008). National Institute of Deafness and Other Communication Disorders. June 2009.http://www.nidcd.nih.gov/health/hearing/usher.asp.

APPENDIX I – PROTEOME OF COCHLEA OF AMES WALTZER MOUSE

- 11 kDa protein
- 29 kDa protein
- similar to ribosomal protein S2 isoform 2
Acan Aggrecan core protein
Acat1 Acetyl-CoA acetyltransferase, mitochondrial
Aco2 Aconitate hydratase, mitochondrial
Acta1 Actin, alpha skeletal muscle
Actb Actin, cytoplasmic 1
Actn1 Alpha-actinin-1
Actn4 Alpha-actinin-4
Actr2 Actin-related protein 2
Actr3 Actin-related protein 3
Ahcy;ENSMUSG00000048538 Adenosylhomocysteinase
Ahnak AHNAK nucleoprotein isoform 1
Ahsg Alpha-2-HS-glycoprotein
Akr1a4 Alcohol dehydrogenase [NADP+]
Akr1b3 Aldose reductase
Alb Serum albumin
Aldh2 Aldehyde dehydrogenase, mitochondrial
Aldh7a1 aldehyde dehydrogenase 7 family, member A1 isoform a
Aldoa Fructose-bisphosphate aldolase A
Alpl Alkaline phosphatase, tissue-nonspecific isozyme
Anpep Aminopeptidase N
Anxa1 Annexin A1
Anxa2 Annexin A2
Anxa5 Annexin A5
Anxa6 annexin A6 isoform b
Apoa1 apolipoprotein A-I
Apod Apolipoprotein D
Apoe Apolipoprotein E
Ar Androgen receptor
Arhgdia Rho GDP-dissociation inhibitor 1
Arhgdia Rho GDP-dissociation inhibitor 1
Arpc1b Arpc1b protein
Arpc4 Actin-related protein 2/3 complex subunit 4
Atp1a1 Sodium/potassium-transporting ATPase subunit alpha-1
Atp1a2 Sodium/potassium-transporting ATPase subunit alpha-2
Atp1a3 Sodium/potassium-transporting ATPase subunit alpha-3
Atp1b1 Sodium/potassium-transporting ATPase subunit beta-1
Atp1b2 Sodium/potassium-transporting ATPase subunit beta-2
Atp1b3 Sodium/potassium-transporting ATPase subunit beta-3
Atp5a1 ATP synthase subunit alpha, mitochondrial
Atp5b ATP synthase subunit beta, mitochondrial
Atp5c1 ATP synthase subunit gamma, mitochondrial
Atp5d ATP synthase subunit delta, mitochondrial
Atp5f1 ATP synthase subunit b, mitochondrial
Atp5h ATP synthase subunit d, mitochondrial
Atp5o;LOC100047429 ATP synthase subunit O, mitochondrial
Bat1a Spliceosome RNA helicase Bat1
Bcat2 Branched-chain-amino-acid aminotransferase, mitochondrial
Bcat2 Branched-chain-amino-acid aminotransferase, mitochondrial
Bdh1 D-beta-hydroxybutyrate dehydrogenase, mitochondrial
Bgn Biglycan
Calr Calreticulin
Camp Putative uncharacterized protein
Canx Calnexin
Capza2 F-actin-capping protein subunit alpha-2
Capzb Isoform 2 of F-actin-capping protein subunit beta
Car2 Carbonic anhydrase 2
Car3 Carbonic anhydrase 3
Cbr1 Carbonyl reductase [NADPH] 1
Cct2 T-complex protein 1 subunit beta
Cct4 T-complex protein 1 subunit delta
Ceacam16 CEA-related cell adhesion molecule 16
Chi3l3 Chitinase-3-like protein 3
Ckb Creatine kinase B-type
Clic1 Chloride intracellular channel protein 1
Cltc Clathrin heavy chain 1
Cndp2 Cytosolic non-specific dipeptidase
Cnp Isoform CNPI of 2',3'-cyclic-nucleotide 3'-phosphodiesterase
Coch Cochlin
Col1a1 Isoform 1 of Collagen alpha-1(I) chain
Col1a2 Collagen alpha-2(I) chain
Col2a1 Isoform 2 of Collagen alpha-1(II) chain
Col4a2 Collagen alpha-2 (IV) chain
Col6a1 Collagen alpha-1(VI) chain
Col6a2 Collagen alpha-2(VI) chain
Col6a3 Col6a3 protein
Col9a2 Collagen alpha-2 (IX) chain
Col9a3 procollagen, type IX, alpha 3
Coro1a Coronin-1A
Cp Ceruloplasmin
Cs Citrate synthase, mitochondrial
Dars Aspartyl-tRNA synthetase, cytoplasmic
Ddost Dolichyl-diphosphooligosaccharide--protein glycosyltranferase 48 kDa subunit
Decr1 2,4-dienoyl-CoA reductase, mitochondrial
Dld Dihydrolipoyl dehydrogenase, mitochondrial
Dpysl2 Dihydropyrimidinase-related protein 2
Dpysl2 Dihydropyrimidinase-related protein 2

Eef1a1 Elongation factor 1-alpha 1
Eef1a2 Elongation factor 1-alpha 2
Eef1b2 Elongation factor 1-beta
Eef1g Elongation factor 1-gamma
Eef2 Elongation factor 2
EG241053 similar to ribosomal protein L12
EG268795 hypothetical protein isoform 2
EG545121 similar to 40S ribosomal protein S14 isoform 1
Eif4a1 Eukaryotic initiation factor 4A-I
Eif4a2 Isoform 1 of Eukaryotic initiation factor 4A-II
Emilin2 EMILIN-2
ENSMUSG00000072432 similar to Glyceraldehyde-3-phosphate dehydrogenase (GAPDH) isoform 1
Epyc Epiphycan
Es1 Liver carboxylesterase N
Espn Isoform 1 of Espin
Etfa Electron transfer flavoprotein subunit alpha, mitochondrial
Etfb Electron transfer flavoprotein subunit beta
Fbxo2 F-box only protein 2
Fga fibrinogen, alpha polypeptide isoform 2
Fgb Fibrinogen beta chain
Flna Isoform 1 of Filamin-A
Fn1 Fibronectin
Fth1 Ferritin heavy chain
Ftl1 Ferritin light chain 1
Gdi2 Isoform 1 of Rab GDP dissociation inhibitor beta
Glud1 Glutamate dehydrogenase 1, mitochondrial
Glul Glutamine synthetase
Gnb1 Guanine nucleotide-binding protein G(I)/G(S)/G(T) subunit beta-1
Gnb2l1 Guanine nucleotide-binding protein subunit beta-2-like 1
Got1 glutamate oxaloacetate transaminase 1, soluble
Got2 Aspartate aminotransferase, mitochondrial
Gpd2 Glycerol phosphate dehydrogenase 2, mitochondrial
Gpi1 Glucose-6-phosphate isomerase
Gsn Isoform 1 of Gelsolin
Gsta4 Glutathione S-transferase A4
Gstm1 Glutathione S-transferase Mu 1
Gstp2 Glutathione S-transferase P 2
H1f0 Putative uncharacterized protein
H2afj Histone H2A.J
H2afy Isoform 1 of Core histone macro-H2A.1
Hadha Trifunctional enzyme subunit alpha, mitochondrial
Hadhb Trifunctional enzyme subunit beta, mitochondrial
Hba-a2;Hba-a1 hemoglobin alpha, adult chain 2
Hbb-b1 Beta-globin
Hhatl Protein-cysteine N-palmitoyltransferase HHAT-like protein
Hist1h1a Histone H1.1
Hist1h1b Histone H1.5
Hist1h1c Histone H1.2
Hist1h1d Histone H1.3
Hist1h1e Histone H1.4
Hist1h2bh Histone H2B type 1-H
Hist2h2ab;Hist2h2ac Histone H2A type 2-C
Hist2h3c1;Hist2h3b;Hist1h3d;Hist1h3e;Hist1h3c;Hist1h3b;Hist1h3f;
Hist2h3c2 Histone H3.2
Hist3h2a Histone H2A type 3
Hk1 Isoform HK1-SA of Hexokinase-1
Hnrnpa2b1 Isoform 3 of Heterogeneous nuclear ribonucleoproteins A2/B1
Hnrnpa3 Isoform 1 of Heterogeneous nuclear ribonucleoprotein A3
Hnrnpd Isoform 2 of Heterogeneous nuclear ribonucleoprotein D0
Hnrnpf Isoform 1 of Heterogeneous nuclear ribonucleoprotein F
Hnrnpu Putative uncharacterized protein
Hsd17b10 Hydroxysteroid (17-beta) dehydrogenase 10
Hsp90aa1 Heat shock protein HSP 90-alpha
Hsp90ab1 MCG18238
Hsp90b1 Endoplasmin
Hspa12a Heat shock 70 kDa protein 12A
Hspa5 78 kDa glucose-regulated protein
Hspa8 Heat shock cognate 71 kDa protein
Hspa9 Stress-70 protein, mitochondrial
Hspd1 Isoform 1 of 60 kDa heat shock protein, mitochondrial
Hspd1 Isoform 1 of 60 kDa heat shock protein, mitochondrial
Hspg2 perlecan
Ibsp Bone sialoprotein 2
Idh2 Isocitrate dehydrogenase [NADP], mitochondrial
Idh3a Isoform 1 of Isocitrate dehydrogenase [NAD] subunit alpha, mitochondrial
Impa1 Impa1 protein
Iqgap1 Ras GTPase-activating-like protein IQGAP1
Iqgap2 Ras GTPase-activating-like protein IQGAP2
Kpnb1 Importin subunit beta-1
Krt1 Keratin, type II cytoskeletal 1
Krt10 keratin complex 1, acidic, gene 10
Krt14 Keratin, type I cytoskeletal 14
Krt15 keratin 15
Krt17 Keratin, type I cytoskeletal 17
Krt2 Keratin, type II cytoskeletal 2 epidermal
Krt42 Keratin, type I cytoskeletal 42
Krt5 Keratin, type II cytoskeletal 5
Krt6a Keratin, type II cytoskeletal 6A
Krt72 Keratin, type II cytoskeletal 72
Krt73 Keratin, type II cytoskeletal 73

Krt75 Keratin, type II cytoskeletal 75
Krt78 keratin Kb40
Lamb1-1 laminin B1 subunit 1
Lamb2 Laminin, beta 2, isoform CRA_a
Lamc1 Laminin subunit gamma-1
Lcn2 Neutrophil gelatinase-associated lipocalin
Lcp1 Plastin-2
Ldha L-lactate dehydrogenase A chain
Ldhb L-lactate dehydrogenase B chain
Lgals1 Galectin-1
Lmna Isoform C of Lamin-A/C
Lmnb1 Lamin-B1
LOC100044223;Eno1;EG433182;EG103324 Alpha-enolase
LOC100045958;Pura Transcriptional activator protein Pur-alpha
LOC100046213;Hist1h2bl;Hist1h2bj;Hist1h2bn;Hist1h2bf Histone H2B type 1-F/J/L
LOC100048522 similar to Cofilin-1
LOC675192;EG668182 hypothetical protein
Lrrc59 Leucine-rich repeat-containing protein 59
Lta4h Leukotriene A-4 hydrolase
Ltf Putative uncharacterized protein
Mapk1 Mitogen-activated protein kinase 1
Mbp Isoform 4 of Myelin basic protein
Mdh1 Malate dehydrogenase, cytoplasmic
Mdh2 Malate dehydrogenase, mitochondrial
Mgp Matrix Gla protein
Mpo Myeloperoxidase
Mpz Myelin P0 protein
Msn Moesin
mt-Co2 Cytochrome c oxidase subunit 2
Myh11 Isoform 1 of Myosin-11
Myh9 Myosin-9
Myl6 Isoform Smooth muscle of Myosin light polypeptide 6
Ndp Norrin
Ndufa8 NADH dehydrogenase [ubiquinone] 1 alpha subcomplex subunit 8
Ndufs1 NADH-ubiquinone oxidoreductase 75 kDa subunit, mitochondrial
Ndufv1 NADH dehydrogenase [ubiquinone] flavoprotein 1, mitochondrial
Nefl Neurofilament light polypeptide
Nefm Neurofilament medium polypeptide
Ngp neutrophilic granule protein
Nid1 Nidogen-1
Oat Ornithine aminotransferase, mitochondrial
Ogdh Isoform 4 of 2-oxoglutarate dehydrogenase E1 component, mitochondrial
OTTMUSG00000000274 similar to ribosomal protein
P4hb Putative uncharacterized protein
Padi2 Protein-arginine deiminase type-2
Pafah1b2 Platelet-activating factor acetylhydrolase IB subunit beta
Pcbp1 Poly(rC)-binding protein 1
Pdhb Pyruvate dehydrogenase E1 component subunit beta, mitochondrial
Pdia3 Protein disulfide-isomerase A3
Pdia4 protein disulfide isomerase associated 4
Pdia6 Putative uncharacterized protein
Pebp1 Phosphatidylethanolamine-binding protein 1
Pfkm 6-phosphofructokinase, muscle type
Pfn1 Profilin-1
Pgam1 Phosphoglycerate mutase 1
Pgd 6-phosphogluconate dehydrogenase, decarboxylating
Pgk1 Phosphoglycerate kinase 1
Pgm1;Pgm2 Phosphoglucomutase-1
Phb Prohibitin
Phb2 Prohibitin-2
Pkm2 Isoform M2 of Pyruvate kinase isozymes M1/M2
Plp1 Isoform 1 of Myelin proteolipid protein
Plxnd1 plexin D1
Pnp1 Purine nucleoside phosphorylase
Ppia Peptidyl-prolyl cis-trans isomerase
Ppib Peptidyl-prolyl cis-trans isomerase B
Prdx1 Peroxiredoxin-1
Prdx2 Peroxiredoxin-2
Prdx5 Isoform Mitochondrial of Peroxiredoxin-5, mitochondrial
Prdx6 Peroxiredoxin-6
Prss2 Anionic trypsin-2
Prx Prx protein
Psat1 Phosphoserine aminotransferase
Ptgds Prostaglandin-H2 D-isomerase
Pygb Glycogen phosphorylase, brain form
Pzp Alpha-2-macroglobulin
Rab10 Ras-related protein Rab-10
Rab14 Ras-related protein Rab-14
Rab5c Ras-related protein Rab-5C
Rab7 Ras-related protein Rab-7a
Rac2 Ras-related C3 botulinum toxin substrate 2
Rph3a1 Isoform 2 of Rab effector Noc2
Rpl10l 60S ribosomal protein L10-like
Rpl11 60S ribosomal protein L11
Rpl14 60S ribosomal protein L14
Rpl15 60S ribosomal protein L15
Rpl3 60S ribosomal protein L3
Rpl4 60S ribosomal protein L4

Rpl5;OTTMUSG00000022843 60S ribosomal protein L5
Rpl6 60S ribosomal protein L6
Rpl7 60S ribosomal protein L7
Rpl7a;EG666669 60S ribosomal protein L7a
Rplp0 60S acidic ribosomal protein P0
Rpn1 Dolichyl-diphosphooligosaccharide--protein glycosyltransferase subunit 1
Rpn2 Dolichyl-diphosphooligosaccharide--protein glycosyltransferase subunit 2
Rps3 40S ribosomal protein S3
Rps3a 40S ribosomal protein S3a
Rps4x 40S ribosomal protein S4, X isoform
Rps7 40S ribosomal protein S7
Rpsa;LOC100045332 40S ribosomal protein SA
S100a8 Protein S100-A8
S100a9 Protein S100-A9
S100b Protein S100-B
Sdha Succinate dehydrogenase [ubiquinone] flavoprotein subunit, mitochondrial
Sept7 cell division cycle 10 homolog
Serpina1c Alpha-1-antitrypsin 1-3
Serpina1d Alpha-1-antitrypsin 1-4
Serpinh1 Serpin H1
Skp1a S-phase kinase-associated protein 1
Slc12a2 solute carrier family 12, member 2
Slc25a11 Mitochondrial 2-oxoglutarate/malate carrier protein
Slc25a12 Calcium-binding mitochondrial carrier protein Aralar1
Slc25a3 Phosphate carrier protein, mitochondrial
Slc25a4 ADP/ATP translocase 1
Slc25a5 ADP/ATP translocase 2
Slc3a2 CD98 heavy chain
Slc4a1 Isoform Erythrocyte of Band 3 anion transport protein
Slc4a11 Sodium bicarbonate transporter-like protein 11
Sod1 Superoxide dismutase [Cu-Zn]
Spna2 Isoform 2 of Spectrin alpha chain, brain
Spnb2 Isoform 2 of Spectrin beta chain, brain 1
Spp1 Osteopontin
Ssb Lupus La protein homolog
Taldo1 Transaldolase
Tcp1 T-complex protein 1 subunit alpha A
Tecta Isoform 1 of Alpha-tectorin
Thbs1 Thrombospondin 1
Tkt Transketolase
Tln1 Talin-1
Tpi1 Triosephosphate isomerase
Tpm3 Isoform 2 of Tropomyosin alpha-3 chain
Tpm4 Tropomyosin alpha-4 chain
Trf Serotransferrin
Tuba1a Tubulin alpha-1A chain
Tuba1b Tubulin alpha-1B chain
Tuba4a Tubulin alpha-4A chain
Tubb2c Tubulin beta-2C chain
Tubb5 Tubulin beta-5 chain
Uba1 Ubiquitin-like modifier-activating enzyme 1
Uba52;Ubc;Ubb;OTTMUSG00000004411;2810422J05Rik hypothetical protein LOC666586
Uqcrc1 Cytochrome b-c1 complex subunit 1, mitochondrial
Uqcrc2 Cytochrome b-c1 complex subunit 2, mitochondrial
Vcl Vinculin
Vcp Transitional endoplasmic reticulum ATPase
Vdac1 Isoform Pl-VDAC1 of Voltage-dependent anion-selective channel protein 1
Vdac2 Voltage-dependent anion-selective channel protein 2
Vdac3 Voltage-dependent anion channel 3
Vim Vimentin
Ywhab Isoform Long of 14-3-3 protein beta/alpha
Ywhae 14-3-3 protein epsilon
Ywhag 14-3-3 protein gamma
Ywhaq Isoform 1 of 14-3-3 protein theta
Ywhaz 14-3-3 protein zeta/delta

Cell Cycle Effects of Simultaneous Treatment with U0126 MEK Inhibitor and Nocodazole

ABSTRACT

This project evaluated the phosphorylation state of intracellular signaling molecules Histone H3 and ERK in Human Umbilical Vein Endothelial Cells (HUVEC) by using iCyte Laser Imaging Cytometry. The hypothesis is that phosphorylation of state-specific antibodies can be used to classify hematological malignancies and monitor drug effects. This project studied the MAPK/ERK (MEK) signaling pathway that is commonly activated in cancer because of mutations involving growth factor receptors.

The effects of nocodazole and MEK 1/2 inhibition by U0126 were analyzed by studying cell cycle arrest as well as the phosphorylation states of ERK and Histone H3. Nocodazole, which disassembles microtubules and interrupts formation of spindle fibers, caused a decrease in G1 and G2/M cell cycle arrest (Fig. 1). U0126 disrupted MEK growth signals, causing the cells to accumulate in G1, G2, and M. In the double treatment (nocodazole plus U0126), cells arrested in G1, G2, and M, and decreased in S phase. Cells moved through mitosis slower in the presence of U0126 and faster when nocodazole was present.

Since the main drug targets are often signaling molecules themselves, studying their pathways will yield drugs with lesser side effects and greater target specificity. The long-term project will utilize a systems biology approach to integrate high-content and high-throughput bioassay data to create models for predicting the potential efficacy, toxicity, and pharmacokinetics of specific pharmaceutical agents in humans.

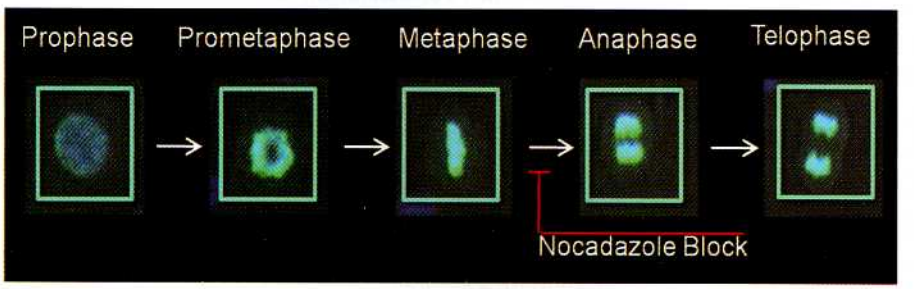

Figure 1: The effects of nocodazole on mitosis. Cells stained with pHistine-H3 (cyan), DAPI (blue), pERK (red).

-Natalie Pyatka-

Nataliya Pyatka is a senior biochemistry student at Case Western Reserve University. In her free time, she enjoys drawing, dancing, reading, and volunteering. At Case, she is a member of WISER (Women in Science and Engineering Roundtable), Discussions, Global Medical Initiative, and HCSL. After graduation, Nataliya plans to pursue an MD degree.

-Acknowledgments-

I thank Dr. Jacobberger for instructing me on my experiments and reviewing my data. In addition, I am very grateful to Tammy Stefan for guiding me though my experiments and training me in research and iCyte procedures. I thank Phil Woost for sharing his knowledge on pERK staining and helping me with the inhibitor concentration calculations. Moreover, I express my deepest gratitude to Anita Merriam for her continued support. This research project was funded by the Center for Stem Cell and Regenerative Medicine (ENGAGE) Program.

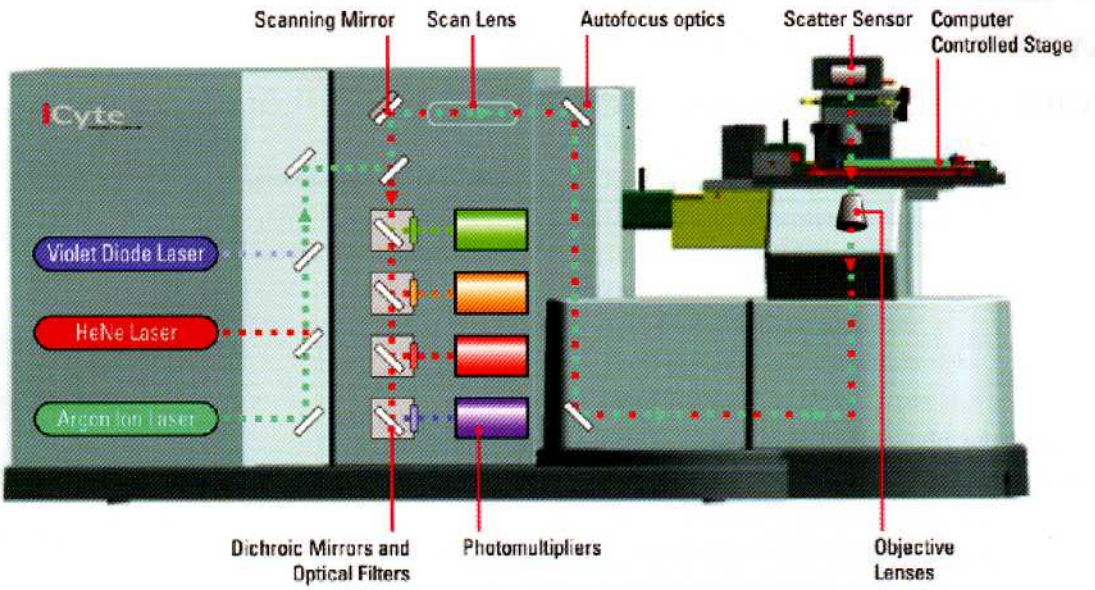

Figure 1: The effects of nocodazole on mitosis. Cells stained with pHistine-H3 (cyan), DAPI (blue), pERK (red).

INTRODUCTION

Since their invention in the 1600's, microscopes have been essential for the advancement of our scientific knowledge. A microscope-based machine called the iCyte Laser Imaging Cytometer is one of the most powerful instruments for cellular analysis. Unlike a simple microscope, the iCyte detects multicolor fluorescence and measures cell properties using lasers and photomultiplier tubes (Fig. 2). Similar to a light microscope, the iCyte displays visual images of the scanned area without destroying the samples. Imaging cytometry provides visual verification and analytical characterization of cellular events (such as apoptosis and cell signaling).

Cytometry measures signals from each cell individually and can correlate two or more parts of data to provide a more complete picture of the cell's behavior. Therefore, cell populations are easily separated based on their statistical differences (such as antibody fluorescence or DNA content). For iCyte analysis, cells can be stained for surface markers because the antibody will form a strong bond to its corresponding antigens. To visualize this bond, a fluorescent tag (such as Alexa Fluor 488-Goat anti-mouse) is used. The presence of proteins like phospho-Histone H3 or phospho-ERK is associated with certain stages of the cell cycle.

The nucleosome, composed of H2A, H2B, H3 and H4 histone proteins, makes up eukaryotic chromatin. Transcription is regulated by chromatin structure modulation. As a result of various stimuli, histones can be phosphorylated, acetylated, methylated, or ubiquitinated. These post-translational modifications have a direct effect on gene expression by making chromatin available (or unavailable) to transcription factors. Chromosome condensation during mitosis is correlated to the phosphorylation of Histone H3 at Ser10. Phosphorylation of Histone H3 begins in late G2, reaches a maximum at metaphase, starts to decrease at metaphase, and is gone at telophase (Hendzel, 1997). Most interphase cells do not show significant levels of phospho-Histone H3. Histone H3's amino-terminus phosphorylation helps to facilitate protein-protein interactions necessary for the binding of trans-acting factors that regulate chromatin condensation and decondensation during mitosis. If the kinase that phophorylates Histone H3 is inhibited, the cell will not be able to enter mitosis (Van Hooser, 1998).

Mitogen-activated protein kinases (MAPKs) are important for cell proliferation, differentiation, and death. The study of MAP kinase cascade is essential for the development of pathway-specific kinase inhibitors and identification of abnormal kinase activity in disease states. Mitogens, growth factors, and cytokines can activate the

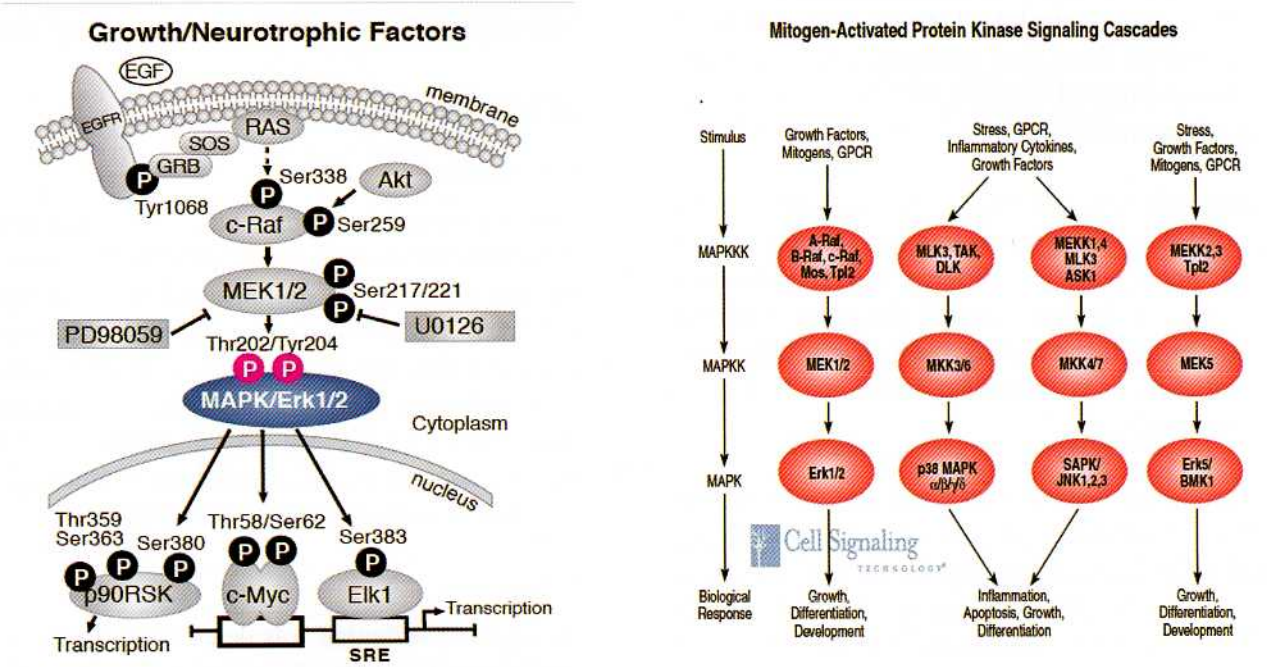

Figure 3: The MAPK/ERK signaling pathway. When stimulated by growth factors, MEK activates cell growth by stimulating transcription. U0126 inhibits MEK phosphorylation and cell proliferation.

p44/42 MAPK (ERK1/2) signaling pathway (Meloche, 2007). Phosphorylation of kinases usually enhances their activities as enzymes and helps to propagate downstream signals. The phosphorylation of ERK1/2 can be used to measure the activation of G protein-coupled receptors. The signaling cascade usually starts the cellular surface and each kinase is activated by being phosphorylated by its upstream member (Fig. 3). To detect the levels of phosphorylated ERK1/2, the mouse antibody phospho-p44/42 MAPK (ERK1/2) is used. It is visible in G1, S, and G2 phases of the cell cycle.

U0126 is a highly selective and potent MEK1&2 inhibitor that causes G1 cell cycle arrest. Decreased MEK activity leads to cessation of cell division but not apoptosis (Blank, 2002). Nocodazole disassembles microtubules, interrupts formation of spindle fibers, and causes fragmentation of the Golgi complex. Thus interphase cells' entry into mitosis is slowed. As an antimitotic agent, nocodazole causes G2/M arrest by binding to tubulin and preventing interchain disulfide links. When nocodazole disassembles microtubules in early prophase, cells return to antephase for 2–4 hours and then ultimately enter mitosis (Rieder, 2002). There is a several hour lag period during which the percentage of mitotic cells does not change due to the disassembled microtubules (Rieder, 2000).

MATERIALS & METHODS

Human Umbilical Vein Endothelial (HUVEC) cell line was cultured in Lonza Endothelial Cell Basal Medium-2 (EBM-2) with 2% fetal bovine serum, FBS, Hydrocortisone, hFGF-B, VEGF, R3-IGF-1, ascorbic Acid, hEGF, GA-100, and heparin. Cells were kept in a humidified incubator with 5% CO2 and 95% air at 37°C.

Samples were prepared in 24-well plates or 4-well chamber slides using 43,000 cells per well. Cells were grown for 2-3 days followed by nocodazole and/or U0126 treatment. 1 mg/mL stock nocodazole was diluted to 3 different concentrations: 50, 100, 200 ng/mL/well. Nocodazole was added and cells were incubated for 0, 2, 4, or 6 hours. For the zero time points, nocodazole was added and immediately aspirated out.

In the experiment with U0126 only, there were four different concentrations: 0, 1, 10, and 100 μM and seven time points: 5, 10, 15, 30, 60, 120, and 360 minutes. The total

treatment volume was 500 µL and each point had triplicate samples. 1 mg of stock U0126 was diluted in 26 µL anhydrous DMSO for a final concentration of 100 µM. When cells were treated with the inhibitor, it was diluted in Lonza culture medium.

In the next experiment with the double treatment (nocodazole and U0126), cells were treated for 30 minutes with 100 ng/mL nocodazole and different U0126 concentrations: 0, 0.4, 2, 10, 50, 100, and 200 µM. Some wells had the inhibitor by itself and nocodazole by itself. There were also control samples with nothing added and each point had quadruplicates.

For the nocodazole experiment (where cells were stained with DAPI DNA probe only), 8 µl of 16% formaldehyde was added to 1 mL culture medium for the total concentration of 0.125%. The cells were then incubated at 37°C for 10 minutes followed by addition of -20°C methanol (1mL per sample). For cells that were to be stained with pERK, the fixation procedure was optimized: formaldehyde was used at 1% concentration was (instead of 0.125%) and the formaldehyde incubation took place at room temperature (26°C). Due to the transient nature of intracellular signaling events, cell fixation was done rapidly to ensure that dephosphorylation did not occur. Methanol acted as a stabilizer to prevent polymerization.

After fixation, two PBS washes (phosphate buffered saline) and one PBS/BSA wash (PBS + bovine serum albumin) were done. The antibodies were diluted with PBA/BSA. 10µl of phospho-Histone H3 (Ser10) antibody and 20 µl of phospho-ERK½ (T202/Y204) antibody was added to 245 µl of PBS/BSA for the total antibody staining volume of 275 µL per sample. The cells were incubated in the dark at 4°C for 60 minutes. All reagents, pipettes, and tubes were kept at 4°C in order to ensure stable temperatures during the staining procedure. Two more PBS/BSA washes were done (with 15 minutes in between each wash) to remove any weakly or nonspecifically bound proteins. The DNA probe was added (DAPI: 0.5 µl/mL concentration, 1mL DAPI/tube) and the samples were run on the iCyte laser imaging cytometer.

In the analysis, the percentage of mitotic cells was measured by phosphorylated Histone H3. ERK phosphorylation monitored the activity of U0126. Cell cycle effects were monitored by phase fractions. Mitotics and new cells were gated out from G2 and G1 and analyzed separately.

RESULTS

Nocodazole

Analysis of cell cycle distribution followed nocodazole treatment. Nocodazole demonstrated a dose and time dependent response: G1 decrease, G2 increase, S decrease, and M increase (Figures 4&5). Prolonged nocodazole treatment also led to an increase in endroreduplicated cells, indicating that DNA replication continued but nuclear division had ceased. 50 and 100 ng/mL nocodazole gave similar results. 200 ng/mL dose was too high because nocodazole's effects seemed to be diminished.

U0126

Cell cycle distribution was determined by measuring the DNA content and the relative amounts of phosphorylated Histone H3. 30 minutes and 10 µM U0126 was determined to be optimal. 1 µM U0126 did not provide the maximum possible cell cycle effects. 10 µM concentration showed strongest the inhibition, but only until 30 minutes (Figure 6&7). Due to U0126's inhibition of MEK, the following effects were observed initially: G1 increase, G2 increase, S increase, M increase, and growth (new cells) decrease. After this time point, the inhibition seemed to have been reversed: G1 decreased, G2 increased, S decreased, M de-

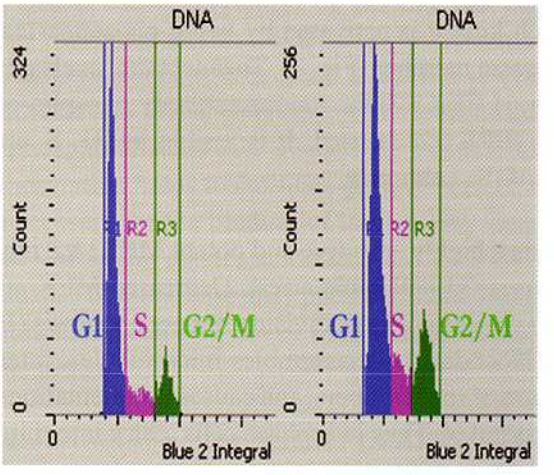

Figure 4: No treatment vs. 4 hr 200 ng/mL nocodazole treatment. The histogram shows the G1 and S area decrease and the G2 increase.

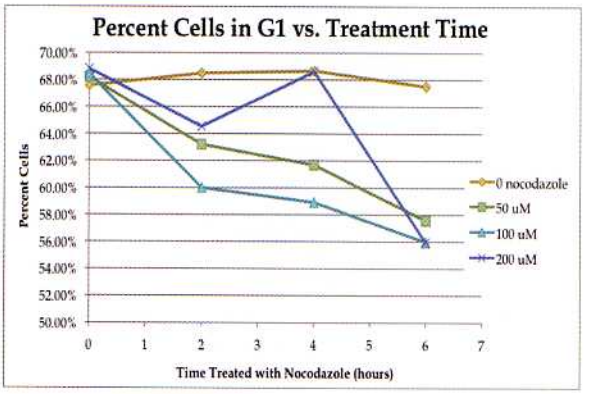

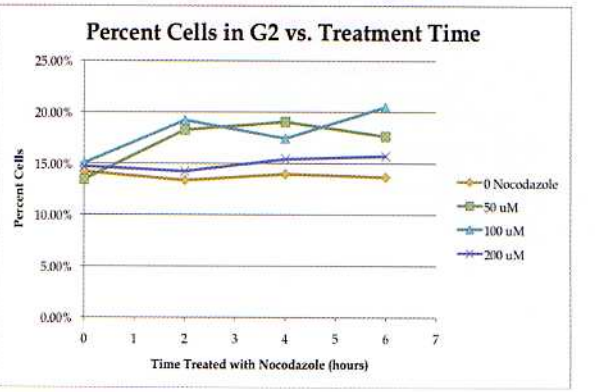

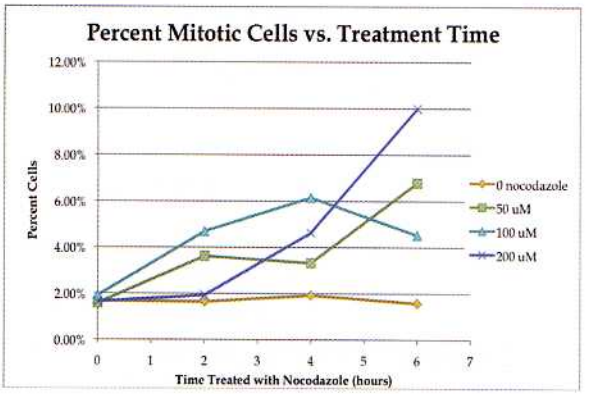

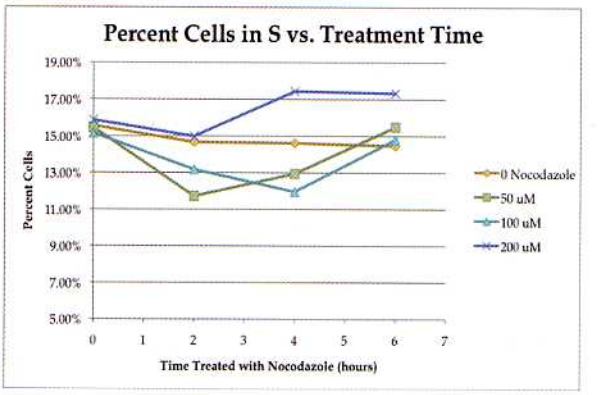

Figure 5: The effects of nocodazole treatment.

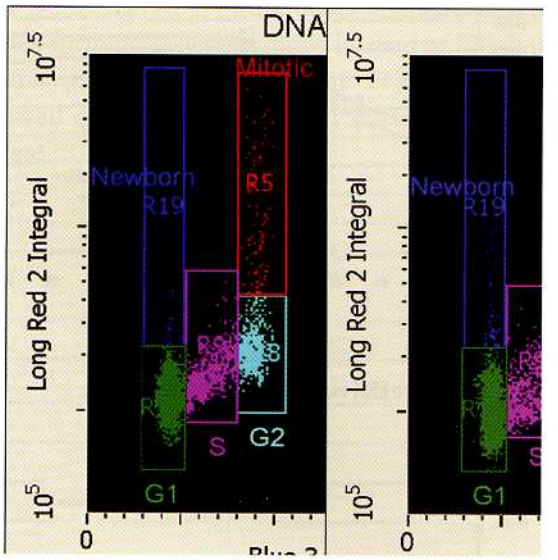

Figure 6: Untreated (left) vs. 10 min, 1μM U0126 treated (right) HUVEC Histone H3 fluorescence. The increase in mitotic, G2 and G1 population due to U0126 is clearly visible.

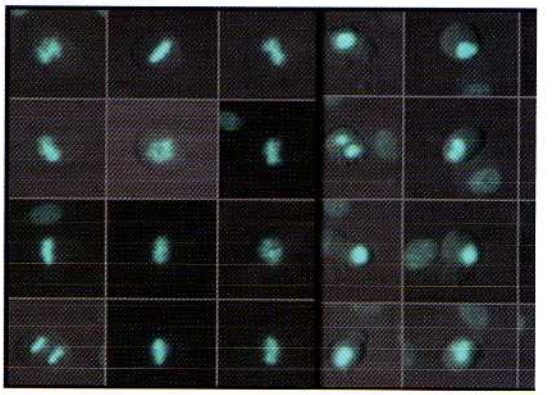

Figure 9: Sample mitotic population of untreated (left) and 4 hour, 100 ng/mL nocodazole treated cells (right). Abnormal morphology can be seen in the treated cells where chromosomes did not line up properly at the metaphase plate during mitosis.

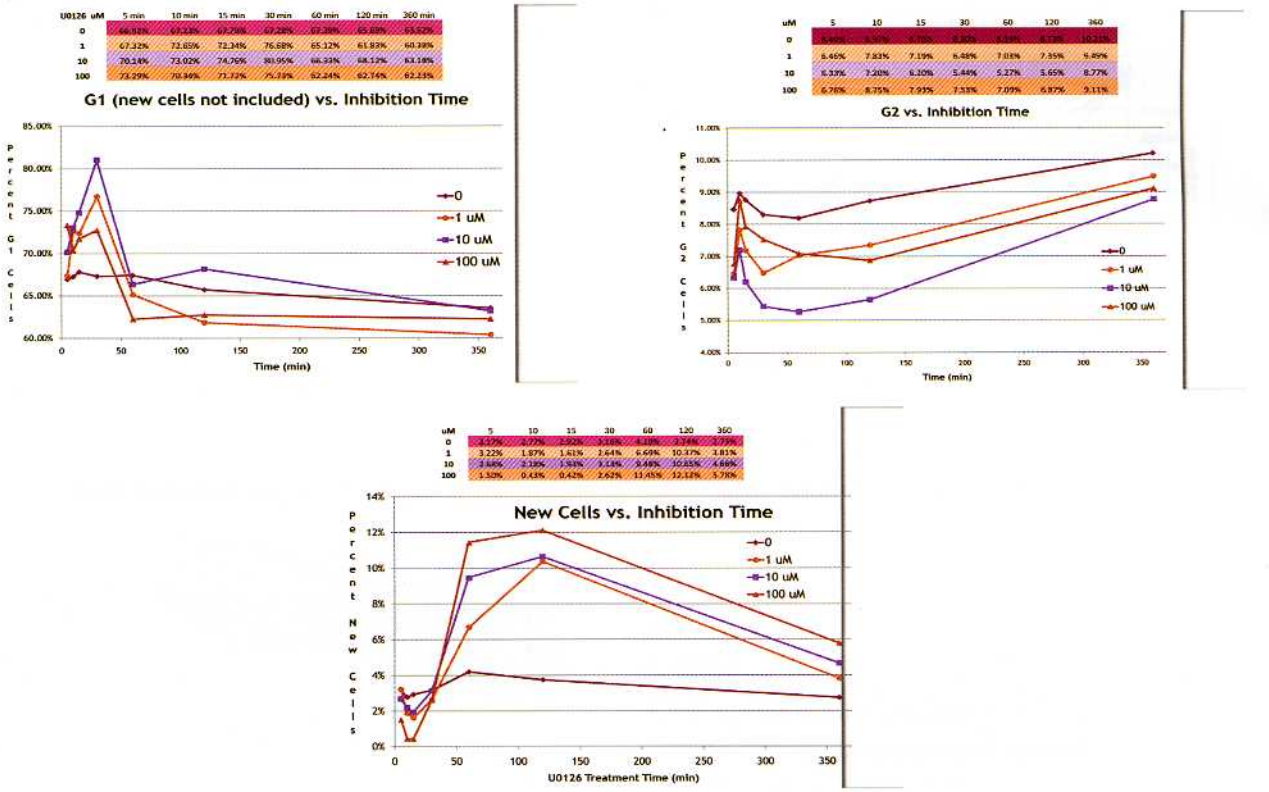

Figure 7: The effects of U0126 treatment.

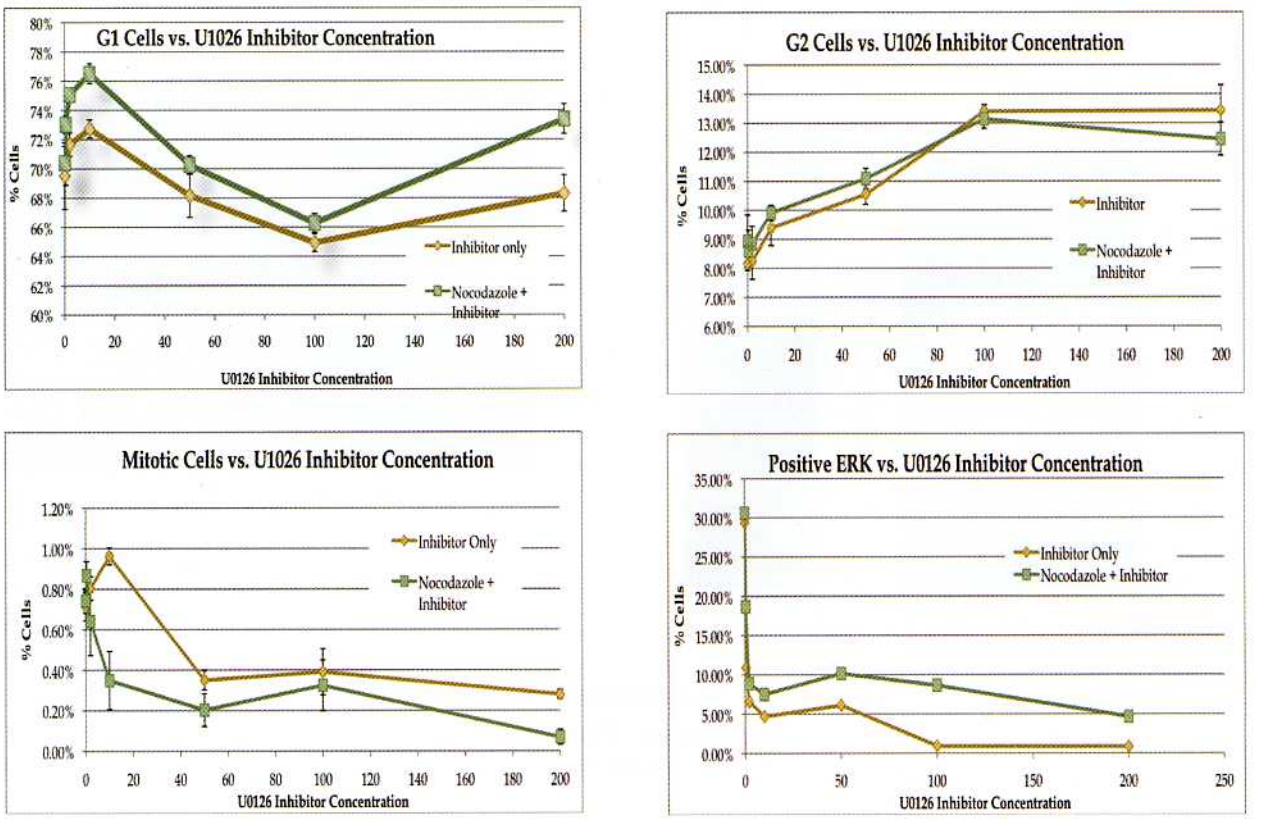

Figure 8: The effects of nocodazole+U0126 treatment.

creased, and growth (new cells) decreased (Figure 7). The ERK signal showed a consistent, dose dependent decrease. These observations demonstrate that cell proliferation was slowed due to decreased growth signals from MEK inhibition.

Nocodazole and U0126

In the double treatment, cells arrested in G1, G2, and M. As a result, S phase decreased (Figure 8). Again, U1026's effects were reversed at concentrations above 10 μM. Nocodazole did not a have dominant effect over U0126 in G2. Cells moved through mitosis slower in the presence of U0126 and faster in the presence of nocodazole. ERK signal was inhibited again, but not as greatly as in the presence of U0126 alone.

DISCUSSIONS & CONCLUSION

From image data it was evident that the ERK signal started at the cellular surface, went to the cytoplasm, and then became localized mostly in the nucleus. This is consistent with ERK's signaling pathway: activating stimuli (such as growth factors) initiate a protein kinase cascade that regulates transcription factors. Based on this information, data analysis focused primarily on nuclear ERK fluorescence.

Nocodazole led to abnormal morphology characterized by chromosomes forming spherical blobs instead of lining up at the metaphase plate (Figure 9, page 21). Cell scatter images showed cells rounding up and starting to detach from the plate.

Up to 50μM U0126 concentrations had potent cell cycle effects. U0126 led to inhibition of transcription because MEK was inhibited and could not stimulate growth. Cells could not get through late G1 phase because MEK growth signals were not present. Thus, S phase decreased because cells were exiting G1 slower and passing through G2 and M at a slower rate.

In the double treatment (nocodazole plus U0126), nocodazole showed an additive, but not synergistic, effect on G1 and S. At higher U0126 concentrations, nocodazole was not strong enough to overcome U0126's effects on G2. G2 showed a consistent increase as a function of U0126. Since the effects of nocodazole are usually not seen until at least 2 hours, the control samples and the samples with nocodazole were not much different.

The study of MAP kinase cascade is essential for the development of pathway-specific kinase inhibitors and the identification of abnormal kinase activity in disease states. Since the main drug targets are often signaling molecules themselves, studying their pathways will yield drugs with lesser side effects and greater target specificity. The long-term project will utilize a systems biology approach to integrate high-content and high-throughput bioassay data to create models for predicting the potential efficacy, toxicity, and pharmacokinetics of specific pharmaceutical agents. Data-driven modeling will also help to identify the mechanism of action of the drugs and improve the utility of early clinical trials.

REFERENCES

Blank, N., Burger, R. 2002. MEK inhibitor U0126 interferes with immunofluorescence analysis of apoptotic cell death. *Cytometry. 48:*179-184.

Givan, A.L. 2001. Flow Cytometry: Second Edition. John Wiley and Sons, Inc., New York.

Hedley, D., Chow, S., Goolsby, C., and Shankey, V. 2008. Pharmacodynamic monitoring of molecular-targeted agents. *Toxicologic Pathology. 36:*133-139.

Hendzel, M.J. 1997. Mitosis-specific phosphorylation of histone H3. *Chromosoma. 106*:348-360.

Jacobberger, J., 1991. Intracellular antigen staining quantitative immunofluorescence. *METHODS: A Comparison to Methods in Enzymology. 3*:207-218.

Jacobberger, J. 2000. Flow cytometric analysis of intracellular protein epitopes. *Immunophenotyping.* 361-405.

Krutzik, P., Nolan, G. 2003. Intracellular phospho-protein staining techniques for flow Cytometry: Monitoring Single Cell Signaling. *Cytometry. 55A*:61-70.

Rieder, C.L., Cole, R. 2000. Microtubule disassembly delays the G2-M transition in vertebrates. *Current Biology. 10:*1067–1070.

Rieder, C.L., Mikhailov, A. 2002. Cell cycle: stressed out of mitosis. *Current Biology. 12*:331-333.

Van Hooser, A., Goodrich, D.W. 1998. Histone H3 phosphorylation. *Journal of Cell Science. 111*:3497-3506.

Breath Play: Sexual and Autoerotic Asphyxiation

-Liz Smith-

Liz Oakley is a senior at Drury University in Springfield, Missouri. She plans to graduate in May, 2010 with a degree in writing as well as minors in psychology, French, and global studies. After graduation, with any luck, she will be spending the 2010-2011 school year teaching English in France through an assistantship with the French Ministry of Culture. Otherwise, she plans to take a year off before applying to graduate school.

In the world of sexual deviance there exist many subcultures. Most of these subcultures of sexual deviance have representations in, and are known to, society. There are websites, magazines, and clubs dedicated to them. Many practices are common knowledge. However, there also exist a few sexually deviant subcultures whose members do not interact with each other. Sexual asphyxia, or autoerotic asphyxiation, is a deviance that is part of the latter (Lowery & Wetli, 1982).

Sexual asphyxia is typically a solitary autoerotic practice, the goal being to obstruct the flow of blood to the brain and induce hypoxia (Friedrich & Gerber, 1994). Practitioners of sexual asphyxia perform the behavior in order to enhance their sexual pleasure through "hypoxic euphoria" induced by strangulation. The strangulation device is designed to cut off the blood flow to the brain and create varying degrees of hypoxic euphoria, giddiness, lightheadedness, and exhilaration which may enhance masturbation sensations and orgasm intensity (Jenkins, 2000). This is a dangerous practice which leads to many accidental fatalities.

The most often used method of strangulation are ligatures such as ropes or belts. Often these are padded to reduce or prevent marks around the neck (Tournel, Hubert, Rougé, Hédouin, & Gosset, 2000). However, asphyxia may also be produced by suspension; plastic bag; face-mask; chest compression; blocking the mouth, nose, or throat; or chemical inhalation (Janssen, Koops, Anders, Kuhn, & Puschel, 2005). The practitioner almost always counts on a safety mechanism or their own reflexes to release them from the strangulation before they lose consciousness. Death occurs when the safety mechanism fails and the practitioner becomes victim.

There have been many compilations made of features of sexual asphyxia related fatalities. While not every feature may appear in every case, several are often present. First of all, there is no apparent wish to die or suicidal intent. Signs that indicate the death was not obviously intended may include body position or presence of protective means, such as padding about the neck. Ropes, belts, and binding materials may be arranged so that constriction of the neck can be controlled voluntarily (Friedrich & Gerber, 1994). The victim is usually partially or completely unclothed. There would most likely be evidence of masturbation or sexual activity, perhaps erotic litera-

-Acknowledgments-

I'd like to thank Dr. Jana Bufkin for her encouragement and input during the writing of this paper. Thanks also to all my wonderful psychology and criminology professors, especially my criminology advisor Dr. Jennie Long for supporting me through my first years at university. I'd also like to acknowledge and thank Mr. Roy Hazelwood for sparking my interest in deviant psychology.

ture or pornography. It is estimated that perhaps 26% of autoerotic asphyxiation cases involve transvestitism (Jenkins, 2000).

Most practitioners of sexual asphyxia are young middle class males with 70% being under the age of 30 (Jenkins, 2000). One study conducted estimates that about 82% of victims are white (Sauvageau & Racette, 2006). Many victims are found to have been intelligent high achievers or workaholics. However, there are no predictors and few signs that a person practices sexual asphyxia. It is unusual for a practitioner to give any signs that would indicate this paraphilia (Lowery & Wetli).

Unlike sadomasochism, exhibitionism, and even pedophilia, those that practice sexual asphyxia rarely engage in their paraphilia with other people, let alone other practitioners. There are several possible reasons for this. First of all, masturbation is almost always a solo practice and not often talked about, and the addition of further paraphilia makes the behavior even less likely to be talked about (Jenkins, 2000). Another reason could be the aforementioned lack of common knowledge of the practice. Even people who do not engage in certain sexual deviances, such as bondage or prostitution, are aware of them and know what they are. This does not seem to be the case with sexual asphyxia.

How then, if sexual asphyxia is so rarely seen in everyday society, do practitioners develop this paraphilia? There have been very few studies done to determine this. The relative absenteeism of this particular paraphilia in mainstream society as well as the unfortunate deaths that make up the majority of scientific studies makes it difficult to investigate the origins of asphyxial behavior.

There have been, of course, several possible causes hypothesized. References to sexual asphyxia have been found in literary sources for centuries; the most commonly referenced being DeSade's Justine (Lowery & Wetli, 1982; Jenkins, 2000; Tournel et al., 2000). The internet and word of mouth are the more generally accepted methods that adolescents and others use to learn of and about sexual asphyxia. However, the reasons behind the incorporation of this paraphilia into recurrent autoerotic behavior are still debated. Psychoanalytic theories such as narcissistic fixation and castration anxiety have been suggested (Lowery; Friedrich & Gerber, 1994).

Unfortunately, most studies of sexual asphyxia center on cases of accidental death, and so few studies have been conducted with living practitioners. One study was performed that examined the histories of five adolescent practitioners of sexual asphyxia. In an admittedly skewed sample, Friedrich and Gerber took the detailed histories of five boys aged 14 to 17 while the boys were receiving therapy at their clinical practice.

As it turns out all five of the boys had suffered childhood physical abuse, childhood sexual abuse, or both. Four out of the five had experienced direct choking at a young age. Four out of the five also displayed other risk taking behaviors such as unprotected sex or alcohol abuse. All five of the boys had experienced some additional trauma, neglect, or loss (such as that of a parent) as well. Prior to experimenting with autoerotic asphyxia, one of the boys was told in detail about his father's death as a fatality of sexual asphyxia.

Friedrich and Gerber concluded that "the etiology of severe and persisting autoerotic asphyxia appears to include the pairing of choking with sexual arousal" (p. 6). The pairing of choking with sexual arousal during childhood trauma facilitated eventual sexual asphyxial behavior. Even though this study is greatly skewed because it was conducted with patients already receiving psychiatric treatment for other concerns it is still very valuable. The overall lack of autobiographical accounts of the practices of sexual asphyxia studies such as the one discussed are useful in understanding the origins of this paraphilia.

It is commonly noted that sexual asphyxia related deaths are likely underreported. At first glance many autoerotic asphyxia related fatalities may appear to be suicide or even homicide. Often victims are found by parents, spouses, or friends who often alter the death scene. This is most likely because of the graphic, shocking, and possibly scandalous circumstances of the death. Also, the police investigators may not be aware of the features of autoerotic asphyxia related deaths and report it as an intentional suicide. (Jenkins, 2000)

Sometimes, however, the details of the death scene make it almost impossible to differentiate between an accident

of sexual asphyxia or intentional suicide. One very unusual case involved a 28 year old muscular dystrophy patient and another party. The man was found naked in a trash container in a sealed plastic sack with strips of tape over his mouth (Koops, Janssen, Anders, & Puschel, 2005). This is an extremely unusual case in which it was not certain whether or not the victim intended on dying. Friends stated that he had talked of suicide, but he had also constructed bizarre and elaborate sexual fantasies as well. One of which was to be enveloped in plastic and put in a trash bin (Koops et al.)

A study investigating solo autoerotic fatalities found that out of 408 published deaths, 374 were caused by sexual asphyxia (Sauvageau & Racette, 2006). Estimates place deaths resulting from autoerotic asphyxiation accounting for as much as 6.5% of adolescent suicides as well as 31% of all adolescent hangings (Jenkins, 2000). Whether this estimation is high or low is hard to say. It cannot be said for certain how many practitioners of sexual asphyxia there are, who they are, or how often they use this form of sexual deviance. Perhaps most importantly, it cannot be said for certain how often sexual asphyxia results in death.

REFERENCES

Friedrich WN, Gerber PN (1994), Autoerotic Asphyxiation: the Development of a Paraphilia. *Journal of the American Academy of Child and Adolescent Psychiatry, 33* (7): 970).

Janssen W, Koops E, Anders S, Kuhn S, Puschel K (2005), Forensic Aspects of 40 Accidental Autoerotic Deaths in Northern Germany. *Forensic Science International*, 147:61.

Jenkins AP, (2000) When Self-Pleasuring Becomes Self-Destruction: Autoerotic Asphyxiation Paraphilia Symposium conducted at the American Alliance for Health, PE, Recreation and Dance National Conference and Exposition, Orlando, Florida.

Koops E, Janssen W, Anders S, Puschel K (2005), Unusual Phenomenology of Autoerotic Fatalities. *Forensic Science International, 147*: 65.

Lowery SA, Wetli CV (1982), Sexual Asphyxia: A Neglected Area of Study. In *Constructions of Deviance* (4th ed., sec. 8, chap. 28) Thomson Wadsworth.

Sauvageau A, Racette S (2006), Autoerotic Deaths in the Literature from 1954 to 2004: A Review. *Journal of Forensic Sciences*, 1(1):140.

Tournel G, Hubert N, Rougé C, Hédouin V, Gosset D (2001), Complete Autoerotic Asphyxiation: Suicide or Accident? *American Journal of Forensic Medicine and Pathology, 22*(2): 180-183.

THANKS TO:

SOURCE

SUPPORT OF UNDERGRADUATE RESEARCH AND CREATIVE ENDEAVORS

http://www.case.edu/provost/source/

Media Board

Media Board is a student group comprised of representatives from each of Case's student media organizations. It promotes responsible forums of student expression in the various media.

Member organizations include The Athenian (Humor Magazine), Case Reserve Review (Literary Magazine), Discussions (Undergraduate Research Journal), Engineering & Science Review, Film Society, Ignite TV, The Observer, Retrospect (Yearbook), and WRUW 91.1 FM.

Since these groups are all student run, they always welcome new members! Any interested students should check out the Media Board website for more information at

http://studentaffairs.case.edu/groups/mediaboard/.

Any media oriented student group interested in becoming a member of Media Board is welcome to apply for membership and should contact the Media Board Chairman at

mediaboard-chairman@case.edu.

How to submit a paper:

1)Visit discussions.case.edu

2) Click and review "Submission Guidelines"

3) Any questions? Email us at discussions@case.edu

4) Information you will need to submit:

-Research advisor
-Your contact information
-A 3rd person biography with a photograph of yourself and 1st person acknowledgements
-Most importantly, your proof-read paper!

How to join DISCUSSIONS:

1) Visit our website to check out past journals—get a general feel for their format

2) Let us know that you're interested. Email us at discussions@case.edu

3) No previous editing experience required, and all majors are welcome

4) You can get involved as a reviewer, copy editor, member of the advertising or design teams, or any combination of the four

CASE WESTERN RESERVE
UNIVERSITY
EST. 1826

10900 Euclid Ave.
Cleveland, Ohio 44106

discussions.case.edu